Comparisons of the local air temperature profiles of serpentine copper-pipe heat exchangers for growing crops

Thiri Shoon Wai[1], **Naoki Maruyama**[1,2], **Napassawan Wongmongkol**[3],
Chatchawan Chaichana[3] and **Masafumi Hirota**[4]

[1]Division of System Engineering, Graduate School of Engineering, Mie University, 1577
  Kurimamachiya-cho, Tsu 514-8507, Japan
[2]Engineering Innovation Unit, Graduate School of Regional Innovation Studies, Mie University,
  1577 Kurimamachiya-cho, Tsu 514-8507, Japan
[3]Department of Mechanical Engineering, Faculty of Engineering, Chiang Mai University, 239
  Huay Kaew Road, Muang Distinct, Chiang Mai 50200, Thailand
[4]Department of Mechanical Engineering, Faculty of Engineering, Aichi Institute of Technology,
  1247 Yachigusa, Yakusa, Toyota 470-0392, Japan

Abstract. This study aims to compare the local air temperature as well as heat transfer of serpentine copper-pipe heat exchanger of different diameters to develop an effective configuration of the heat exchanger for growing crops inside greenhouses. The local air temperature indicates the air temperature close to that of the growing crops. Cooling experiments were conducted using a heat exchanger. The performance of the heat exchanger with different outer pipe diameters was analyzed for 12.7 mm and 15.88 mm. The inlet fluid temperature and flow rate were varied for the experimental conditions. The inlet fluid temperature ranged from −5 °C to 10 °C whereas the fluid flow rate ranged from 0.3 L/min to 3.0 L/min. The experimental data such as the local air temperature, inlet and outlet fluid temperatures, surface pipe temperatures, and pressure drop were measured. The relative humidity was monitored by observing the water droplets on the surface of the pipes. The average local air temperature reduction of the area below of the serpentine heat exchangers can reach up to 9.0 ºC and 10 ºC for the diameters of 12.7 mm and 15.88 mm, respectively. The pressure drop in the serpentine heat exchanger of diameter 15.88 mm was approximately half of that in the heat exchanger of diameter 12.7 mm. This may decrease the pumping power and lead to reduction in energy consumption of a heat exchanger of diameter 15.88 mm compared with that of an exchanger of diameter 12.7 mm diameter. Therefore, the advantages and disadvantages of each type of heat exchanger must be considered when selecting a suitable heat exchanger for greenhouse farming.

Nomenclature

A_s	outer surface area of the copper pipe (m²)		*Greek symbols*	
c_p	specific heat of fluid [J/(kg.K)]		ρ	fluid density (kg/m³)
d_{inside}	inner diameter of the copper pipe (m)		v	fluid velocity (m/s)
$d_{outside}$	outer diameter of the copper pipe (m)		μ	dynamic viscosity of the fluid (Pa.s)
ΔP	pressure drop in the heat exchanger (kPa)			
$\dot{q}_t$	heat transfer from the copper pipe surfaces (W/m²)			
Re	Reynolds number (Dimensionless)			

T_{inlet}	inlet fluid temperature (℃)	*Subscripts*	
T_{outlet}	outlet fluid temperature (℃)	*a*	air
T_{lair,avg_be}	average local air temperature below the heat exchanger (℃)	*ab*	above
		avg	average
T_{lair,avg_ab}	average local air temperature above the heat exchanger (℃)	*be*	below
		f	fluid
T_{room}	room air temperature (℃)	*lair*	local air
ΔT_f	fluid temperature difference (℃) $= T_{outlet} - T_{inlet}$ (℃)		
ΔT_a	air temperature reduction (℃)		
$\dot{V}$	fluid flow rate (L/min), (m³/s)		

1.   Introduction

The significance of the modern greenhouse agricultural sector has been increasing in recent years owing to the growth of the global population and the increasing demand for food [1,2]. Greenhouse farming enables the year-round production of crops by avoiding extreme weather conditions [3,4]. Maintaining a suitable environmental climate is essential for supporting plant growth and productivity in greenhouse farming. Extensive research has been conducted on cooling systems, including natural ventilation, forced ventilation, evaporative cooling, and combined cooling systems [5–9]. These systems control the air temperature throughout the greenhouse farming area. Low air temperatures can be obtained in tropical regions with intensive cooling systems, such as air-conditioning systems. However, these systems require a considerable amount of energy to create a suitable environment for crops [10]. In addition, heat exchangers are widely utilized in various industrial applications such as power plants, heating, ventilation, and air conditioning systems [11–15]. In greenhouse crop cultivation, earth-air heat exchangers are one of the methods to provide the environmental control for crops [16–19]. The earth air heat exchangers use underground pipes under certain depth of the soil and carry indoor or outdoor air into the pipes. The temperature difference between the soil and air can be applied to substitute the heated or cooled air in the greenhouse. In this way, the earth air heat exchanger system provides air temperature control in the greenhouse. However, this system also supplies air temperature to the whole greenhouse area. Extensive research has been conducted on greenhouse designs and cooling systems to obtain an appropriate environment for crops by considering the entire greenhouse area.

However, there is limited research on local cooling climate control, which focuses only on the plants. Heat sensitive crops such as strawberries require an air temperature between 20–25 ℃ and 10–12 ℃ during the day and night, respectively, which presents a major drawback for their cultivation in tropical regions [20]. Therefore, local cooling climate control has been proposed for greenhouse farming to reduce the energy consumption. Furthermore, suitable heat exchanger configurations must be developed for smart greenhouse farming.

This study aims to compare the local air temperature as well as heat transfer of serpentine copper-pipe heat exchangers of different diameters to develop a suitable configuration of the heat exchanger for growing crops inside greenhouses. The outer diameters of the copper pipe were 12.7 mm and 15.88 mm and cooling experiments were implemented in a laboratory room. The experimental conditions were altered through changes in both the inlet fluid temperature and the flow rate. The inlet fluid temperature ranged from −5 °C to 10 °C whereas the fluid flow rate ranged from 0.3 L/min to 3.0 L/min.

2.   Methodology

2.1.   Experimental setup

Figure 1 depicts the configuration of the serpentine copper-pipe heat exchanger with a width and length of 700 mm and 253 mm, respectively, except for the bend areas. The thickness of the copper pipes is 0.8 mm. Each pipe was assembled in a U-bend and these U-bends were covered with insulation. The pitch of each copper pipe is 50 mm. Types 1 ($d_{outside} = 12.7$ mm) and 2 ($d_{outside} = 15.88$ mm) heat exchangers with the same pitch were tested. The experiments were conducted by changing the pipe

diameter of the heat exchanger in the same test section area. An insulation board was used to separate the experimental system from the room. In this study, we consider strawberry crops for greenhouse farming, and a heat exchanger is installed above the plants for local cooling. Figure 2 presents an overview of the experimental system. The dimensions of the experimental area are 1.4 m (W) × 0.7 m (D) × 1.0 m (H).

Heat exchanger's specification		
Parameter	Type 1	Type 2
	Dimension	
Outer pipe diameter (mm)	12.7	15.88
Pitch (mm)	50	50
Pipe thickness (mm)	0.8	0.8
No. of pipes	15	15
Pipe surface area (m^2)	0.151	0.189
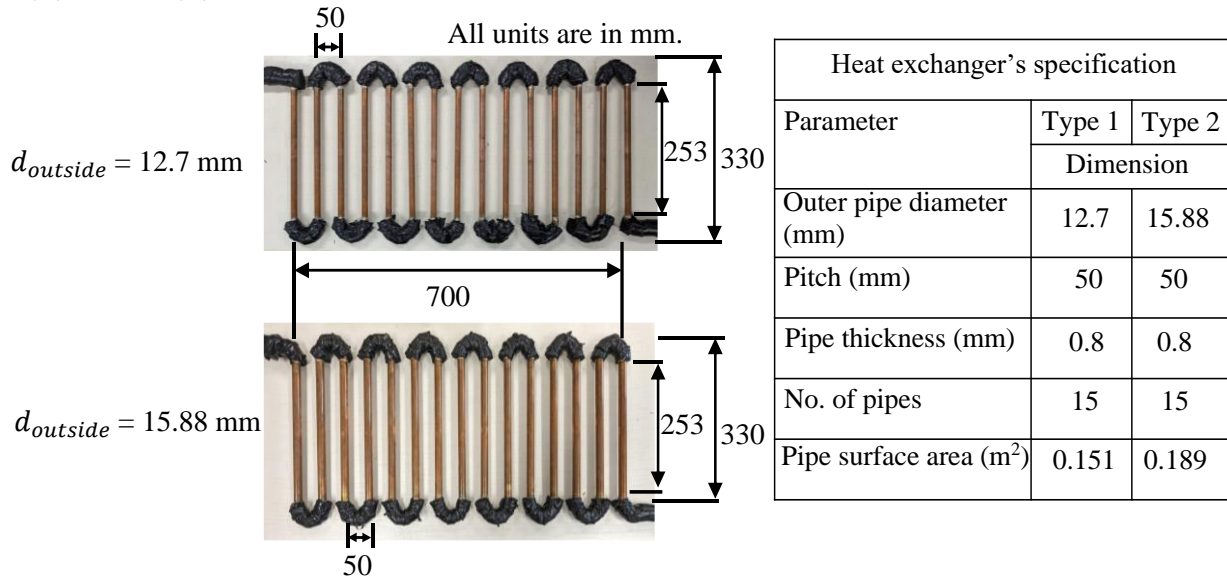
Figure 1. Serpentine copper-pipe heat exchanger configuration.
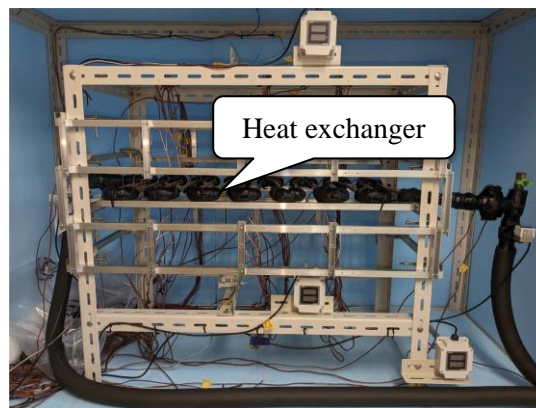
Figure 2. Serpentine copper-pipe heat exchanger experimental system setup.

2.2. Data collection
The air temperatures at the area below and above the heat exchanger were measured to analyze the local air temperature profiles. Figure 3 depicts the vertical air temperature measurements around the heat exchanger. There were three horizontal layers below and above the heat exchanger. We focus on the area below the heat exchanger and the area above it was used as a reference. The layers below the heat exchanger were located 50 mm, 100 mm, and 150 mm from the center of the heat exchanger, as shown in Figure 3(a). The above layers are symmetrical to those below, and are −50 mm, −100 mm, and −150 mm away from the center of the heat exchanger, as shown in Figure 3(b). There were nine thermocouples in each horizontal layer, resulting in 54 thermocouples in the six layers. Furthermore, the vertical uncertainty of the thermocouple's positions in each horizontal layer was ±2 mm.

(a)   (b)

Figure 3. Measurement of air temperature vertically: areas (a) below and (b) above the heat exchanger.

Figure 4 depicts the layout of the experimental system. The system included a serpentine heat exchanger, globe valves to control the flow rates, a chiller to cool the fluid, thermocouples for surface, inside room air, outside air and local air temperature measurements, resistance thermal detectors for inlet and outlet fluid temperature measurement, and a pressure difference sensor to measure the pressure drop of the heat exchanger. Humidity sensors were introduced for reference.

Three data loggers were used to collect the experimental data. T-type thermocouples have a measurement accuracy of $\pm$ 0.2 ºC, and they are calibrated with the reference temperature. The resistance thermal detectors were calibrated based on their initial temperature differences and have a measurement accuracy of $\pm$ 0.02 ºC.
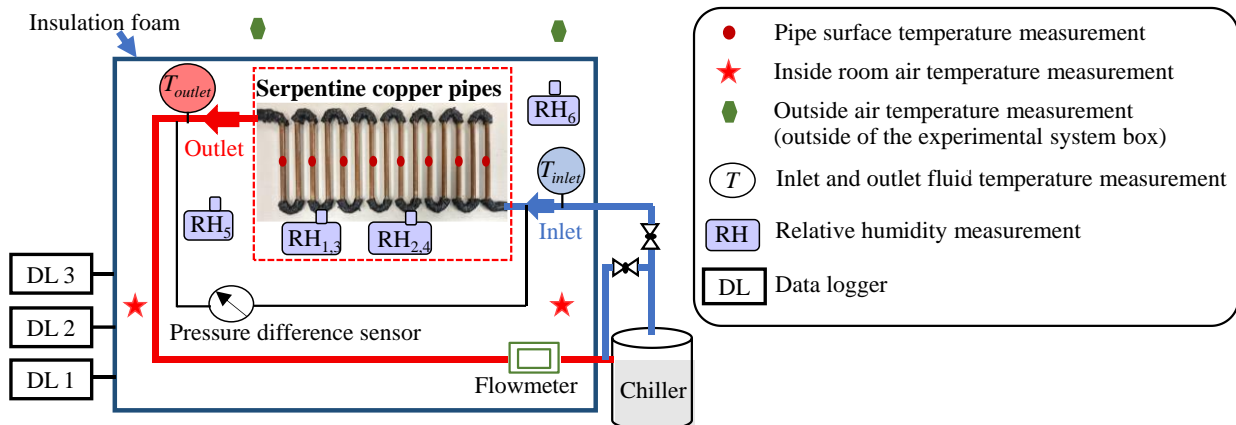
Figure 4. Experimental system layout.

2.3. Experimental conditions

The inlet fluid temperature and fluid flow rate were varied for experimental conditions. The inlet fluid temperature ranged from −5 ºC to 10 ºC whereas the flow rate ranged from 0.3 to 3.0 L/min for both the heat exchangers, as can be seen in Table 1. The Reynolds numbers ranged from 63 to 1,394 and 50 to 1,100 for pipe diameters of 12.7 mm and 15.88 mm, respectively. We used a mixture of water (60% by volume) and ethylene glycol (40% by volume) as the working fluid to reduce the freezing point of water. The experimental data were collected at the outside air temperature of 25 ºC.

Table 1. Experimental conditions for both heat exchangers.

No.	Inlet fluid temperature T_{inlet} (°C)	Fluid flow rate $\dot{V}$ (L/min)	No.	Inlet fluid temperature T_{inlet} (°C)	Fluid flow rate $\dot{V}$ (L/min)
1		0.3	21		0.3
2		0.5	22		0.5
3		0.7	23		0.7
4		0.9	24		0.9
5	−5	1.1	25	5	1.1
6		1.3	26		1.3
7		1.5	27		1.5
8		2.0	28		2.0
9		2.5	29		2.5
10		3.0	30		3.0
11		0.3	31		0.3
12		0.5	32		0.5
13		0.7	33		0.7
14		0.9	34		0.9
15	0	1.1	35	10	1.1
16		1.3	36		1.3
17		1.5	37		1.5
18		2.0	38		2.0
19		2.5	39		2.5
20		3.0	40		3.0

The Reynolds number (Re) is calculated as:

$$Re = \frac{\rho v d_{inside}}{\mu} \tag{1}$$

where ρ is the fluid density (kg/m³), v is the velocity of the fluid (m/s), d_{inside} is the inner diameter of the copper pipe (m), and μ is the fluid dynamic viscosity (Pa.s).

The heat transfer was determined from the data obtained under steady-state conditions, as follows:

$$\dot{q}_t = \frac{\rho \dot{V} c_p (T_{outlet} - T_{inlet})}{A_s} \tag{2}$$

where $\dot{q}_t$ is the heat flux from the copper pipe surfaces (W/m²), $\dot{V}$ is the volumetric flow rate of fluid (m³/s), c_p is the fluid specific heat [J/(kg.K)], A_s is the outer surface area of the copper pipe without the U-bends (m²), and T_{inlet} and T_{outlet} are the inlet and outlet fluid temperatures (°C), respectively.

3. Results and discussion

In this study, the local air temperature indicates the air temperature close to the growing crops. The analysis of the heat flux within the heat exchanger was conducted using a flow rate ranging from 0.3 to 1.3 L/min. The heat flux assessment of the flow rate higher than 1.5 L/min was omitted owing to the low accuracy of the measured fluid temperature difference (ΔT_f).

3.1. Local air temperature profiles and air temperature reduction

Figure 5 presents comparisons of the average local air temperature profiles at each vertical distance around the Type 1 and Type 2 serpentine copper-pipe heat exchangers. The local air temperatures in each horizontal layer of the nine thermocouples were averaged. Figure 5(a) and (b) present the average local air temperature profile of areas below and above the heat exchanger, respectively, at a flow rate of $\dot{V} = 0.9$ L/min as a reference for all the inlet fluid temperatures. The average local air temperatures of each layer in the area below and above the heat exchanger are denoted as T_{lair,avg_be} and T_{lair,avg_ab}, respectively.

The T_{lair,avg_be} values of both the heat exchangers at each layer are approximately 12 °C, 15 °C, 17 °C, and 20 °C with inlet fluid temperatures of −5 °C, 0 °C, 5 °C, and 10 °C, respectively. According to Figure 5(b), the T_{lair,avg_ab} values of both the heat exchangers range from 14 °C to 21 °C for the inlet fluid temperatures of −5 °C, 0 °C, 5 °C, and 10 °C. A comparison of Figure 5(a) and (b) shows that T_{lair,avg_be} was lower than T_{lair,avg_ab} for both types of heat exchangers. This is attributed to the buoyancy force which generates downward airflow.

It can be observed that the surrounding air temperature near both types of heat exchangers is decreased. This confirms that both the heat exchangers can provide effective cooling, particularly in the areas below them.

T_{lair,avg_be}	$d_{outside}$	T_{inlet} (°C)				Inside room air temperature (°C)
		−5 °C	0 °C	5 °C	10 °C	
Type 1	12.7 mm	–⊖–	–◇–	–△–	–☐–	———
Type 2	15.88 mm	–●–	–◆–	–▲–	–■–	

(a)

T_{lair,avg_ab}	$d_{outside}$	T_{inlet} (°C)				Inside room air temperature (°C)
		−5 °C	0 °C	5 °C	10 °C	
Type 1	12.7 mm	⊖	◇	△	☐	———
Type 2	15.88 mm	●	◆	▲	■	

(b)
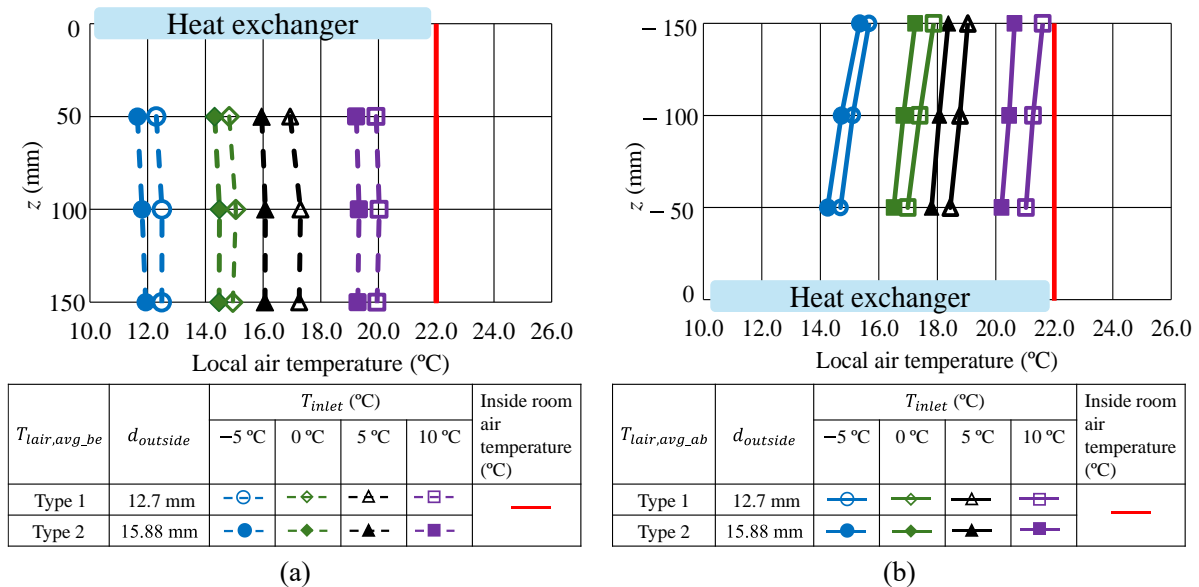
Figure 5. Local air temperature profiles in the areas (a) below and (b) above both types of heat exchangers at $\dot{V}$ = 0.9 L/min.

Figure 6 depicts the average local air temperature reduction from the inside room air temperature of the areas below and above the two types of heat exchangers under steady-state conditions for all the inlet fluid temperatures under flow rate ranging from 0.3 L/min to 1.3 L/min. The local air temperatures of the three layers below and above were averaged. Subsequently, the average local air temperature reductions below and above the initial room air temperature were analyzed. At the flow rate of 0.3 L/min and inlet fluid temperature of −5 °C, the average local air temperature reduction of Type 1 ($\Delta T_{a-be\_12.7}$) and ($\Delta T_{a-ab\_12.7}$) are approximately 7.0 °C and 4.5 °C below and above, respectively. Conversely, in the case of Type 2, $\Delta T_{a-be\_15.88}$ and $\Delta T_{a-ab\_15.88}$ are approximately 9.0 °C and 6.0 °C, respectively.

When the inlet fluid temperature increases from −5 °C to 10 °C, the average local air temperature reductions significantly decrease for both the heat exchangers. Although the flow rate increased, the average local air temperature reduction was insignificant after 0.7 L/min. It can be concluded that the local air temperature can be reduced, even with a low flow rate. As the inlet fluid temperature decreased, the local air temperature decreased from its initial value. This implies that the inlet fluid temperature has a greater impact on the local air temperature compared to the flow rate.

Figure 6. Comparisons averaged air temperature reduction in the areas below and above the Type 1 and Type 2 heat exchanger from their initial air temperature.

3.2. *Pressure drop*

Figure 7 depicts the pressure drop in the two types of heat exchangers for flow rate ranging from 0.3 to 1.3 L/min at all the inlet fluid temperatures. Figure 7(a) and (b) present the pressure drops in the Type 1 and Type 2 heat exchangers, respectively. The pressure drop decreased as the inlet fluid temperature increased, as shown in Figure 7. This is due to the decrease in the fluid viscosity when the inlet fluid temperature increases. However, the pressure drop increased when the flow rate increased.

A comparison of Figure 7(a) and (b) shows that the decrease in pressure drop is related to an increase in the diameter of the copper pipe. The pressure drop in the Type 2 heat exchanger is lower than that in the Type 1 heat exchanger as the pressure drop corresponds to the diameter of the copper pipe. The pressure drop ranges from 0.3 kPa to 3.0 kPa for both types of heat exchangers. The pressure drop in the Type 2 heat exchanger was approximately half of that in the Type 1 heat exchanger. Based on the experimental results, a Type 2 heat exchanger was selected as it presented a lower pressure drop than the Type 1 heat exchanger.

Figure 7. Pressure drop under all experimental conditions for (a) Type 1 and (b) Type 2 heat exchangers.

3.3. Heat flux in the heat exchanger

Figure 8 depicts the outlet and inlet fluid temperature difference (ΔT_f) of both types of heat exchangers at all the inlet fluid temperatures under a flow rate ranging from 0.3 L/min to 1.3 L/min. ΔT_f decreased markedly with the increase in the flow rate. This indicates that ΔT_f correlates to the flow rate. Furthermore, the ΔT_f values were almost identical for both types of heat exchangers for all the experimental conditions. At a low flow rate of 0.3 L/min, the ΔT_f value is higher than those at other flow rates. This could be attributed to the longer contact time between the fluid and the pipe surface in the heat exchangers. The ΔT_f values range from 2.5 ℃ to 0.2 ℃ for flow rates from 0.3 L/min to 1.3 L/min at all the inlet fluid temperatures.
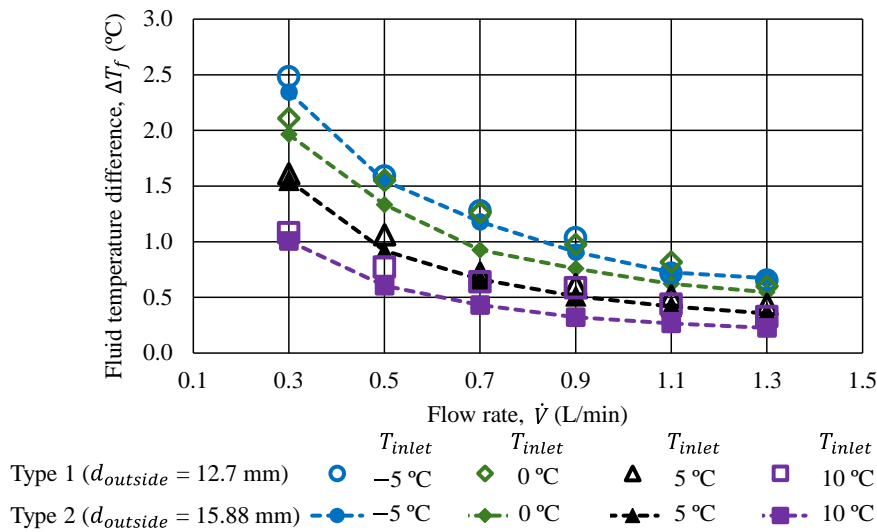
Figure 8. Inlet and outlet fluid temperature difference at all experimental conditions for both types of heat exchangers.

Figure 9 presents a comparison of the heat flux in the Type 1 and Type 2 heat exchangers. The heat flux ($\dot{q}_t$) was calculated using Eq. (2); it presents the relationship between ΔT_f and flow rate. At a flow rate of 0.3 L/min for the Type 1 heat exchanger, $\dot{q}_t$ was approximately 330 W/m^2 at an inlet fluid temperature of −5 ℃ and the minimum $\dot{q}_t$ was approximately 150 W/m^2 at an inlet fluid temperature of 10 ℃. Conversely, for Type 2 heat exchanger, $\dot{q}_t$ was about 250 W/m^2 at −5 ℃ inlet fluid temperature and $\dot{q}_t$ was approximately 100 W/m^2 at 10 ℃ inlet fluid temperature. The heat flux steadily increased with the flow rate.

The overall heat flux in the Type 1 heat exchanger was higher than that in the Type 2 heat exchanger. This is attributed to the thin thermal boundary layer of the Type 1 heat exchanger owing to the higher fluid velocity than that of the Type 2 heat exchanger at the same flow rate. Consequently, the heat flux of the Type 1 heat exchanger was higher than that of the Type 2 heat exchanger.
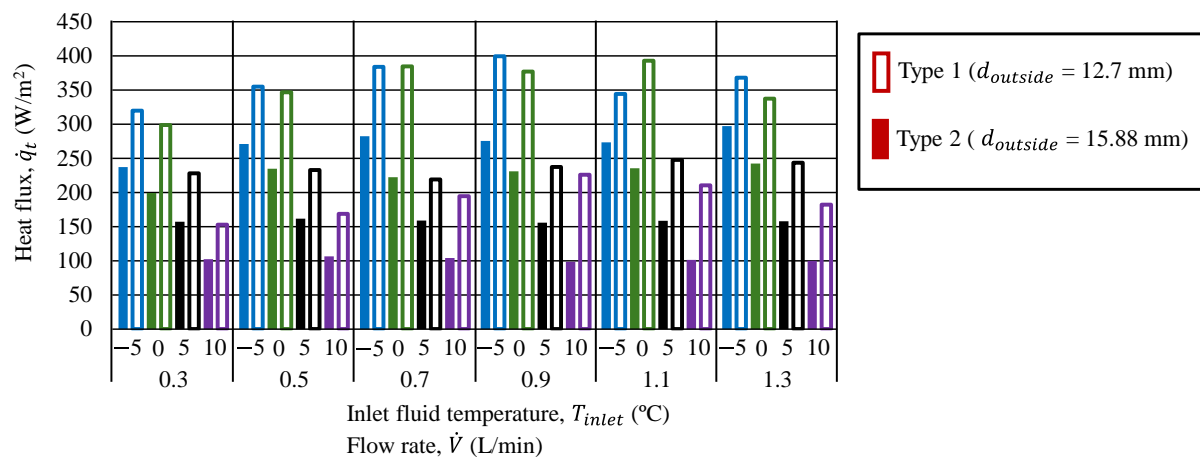
Figure 9. Heat flux at all experimental conditions for both types of heat exchanger.

4. Conclusion

In this study, we compared the local air temperature profiles of serpentine copper-pipe heat exchangers with different diameters to develop a suitable configuration for growing crops in greenhouse farming. The inlet fluid temperature and flow rate in the heat exchanger were varied for the experimental conditions. At an inlet fluid temperature of −5 °C, a maximum local air temperature reduction of 9.0 °C from the initial air temperature can be obtained in the area below the Type 1 heat exchanger. However, the local air temperature can be reduced by up to 10 °C from the initial air temperature in the area below the Type 2 heat exchanger. The results indicate that both the heat exchangers can provide effective cooling, particularly in the areas below them. Furthermore, the local air temperatures can be reduced even at low flow rates. A lower flow rate could potentially be adequate as the local air temperatures show insignificant change after a flow rate of 0.7 L/min.

The pressure drop in the Type 2 heat exchanger was approximately half of that in the Type 1 heat exchanger. This may decrease the pumping power required and lead to a reduction in the energy consumption of the heat exchanger when Type 2 is chosen over Type 1. However, the larger pipe diameter of the Type 2 heat exchanger may have created more sunlight shadows on the plantation. The cost of a larger pipe diameter for Type 2 may be higher than that for Type 1. Therefore, the advantages and disadvantages of each type of heat exchanger must be considered when selecting a suitable heat exchanger for greenhouse farming. This heat exchanger system and methodology can also be applied for local heating in cold-climate regions.

5. References

[1] Vermeulen S J, Aggarwal P K, Ainslie A, Angelone C, Campbell B M, Challinor A J et al 2012 Options for support to agriculture and food security under climate change *Environ. Sci. Policy* **15** pp. 136–144

[2] Ouazzani Chahidi L, Fossa M, Priarone A, and Mechaqrane A 2021 Greenhouse cultivation in Mediterranean climate: Dynamic energy analysis and experimental validation *Therm. Sci. Eng. Prog.* **26** pp. 1–9

[3] Sahdev R K, Kumar M, and Dhingra A K 2019 A comprehensive review of greenhouse shapes and its applications *Front. Energy* **13** pp. 427–438

[4] Morshed W, Abbas L, and Nazha H 2022 Heating performance of the PVC earth-air tubular heat exchanger applied to a greenhouse in the coastal area of west Syria: An experimental study *Therm. Sci. Eng. Prog.* **27** pp. 1–8

[5] Tawalbeh M, Aljaghoub H, Alami A H, and Olabi A G 2023 Selection criteria of cooling technologies for sustainable greenhouses: A comprehensive review *Therm. Sci. Eng. Prog.* **38** pp. 1–26

[6]   Akrami M, Salah A H, Javadi A A, Fath H E S, Hassanein M J, Farmani R et al 2020 Towards a sustainable greenhouse: Review of trends and emerging practices in analysing greenhouse ventilation requirements to sustain maximum agricultural yield *Sustain.* **12** pp. 1–18

[7]   Kolokotsa D, Saridakis G, Dalamagkidis K, Dolianitis S, and Kaliakatsos I 2010 Development of an intelligent indoor environment and energy management system for greenhouses *Energy Convers. Manag.* **51** pp. 155–168

[8]   Plessis E du, Workneh T, and Laing M 2015 Greenhouse Cooling Systems and Models for Arid Climate *BT - Sustainable Agriculture Reviews* **18** pp. 181–215

[9]   Soussi M, Chaibi M T, Buchholz M, and Saghrouni Z 2022 Comprehensive Review on Climate Control and Cooling Systems in Greenhouses under Hot and Arid Conditions *Agronomy* **12** pp. 1–31

[10]   Banakar A, Montazeri M, Ghobadian B, Pasdarshahri H, and Kamrani F 2021 Energy analysis and assessing heating and cooling demands of closed greenhouse in Iran *Therm. Sci. Eng. Prog.* **25** pp. 1–7

[11]   Cengel Y A and Ghajar A J 2020 Heat and mass transfer fundamentals and applications 5th Ed. McGraw Hill Education

[12]   Kurapalli S M, Ramareddy S, Shantappa G S 2023 Experimental Study on the Effect of TiO_2–Water Nanofluid on Heat Transfer and Pressure Drop in Heat Exchanger with Varying Helical Coil Diameter *J Adv Res Fluid Mech Therm Sci.* **107** pp. 50–67

[13]   Chen Q, Xu G, Xia P 2021 The performance of a solar-driven spray flash evaporation desalination system enhanced by microencapsulated phase change material *Case Stud Therm Eng.* **27** pp. 1–15

[14]   Master B I, Chunangad K S, Boxma A J, Kral D, Stehlík P 2006 Most frequently used heat exchangers from pioneering research to worldwide applications *Heat Transf Eng.* **27** pp. 4–11

[15]   Kabeel A E, El-Said E M S 2014 A hybrid solar desalination system of air humidification, dehumidification and water flashing evaporation: Part II. Experimental investigation *Desalination* **341** pp 50–60

[16]   Xiao J, Wang Q, Wang X, Hu Y, Cao Y, Li J 2023 An earth-air heat exchanger integrated with a greenhouse in cold-winter and hot-summer regions of northern China: Modeling and experimental analysis *Appl Therm Eng* **232** pp. 1–17

[17]   Hamdane S, Pires L C C, Silva P D, Gaspar P D 2023 Evaluating the Thermal Performance and Environmental Impact of Agricultural Greenhouses Using Earth-to-Air Heat Exchanger: An Experimental Study *Appl Sci.* **13** pp. 1–13

[18]   Zajch A, Gough W A 2021 Seasonal sensitivity to atmospheric and ground surface temperature changes of an open earth-air heat exchanger in Canadian climates *Geothermics* **89** pp. 1–11

[19]   Bordoloi N, Sharma A, Nautiyal H, Goel V 2018 An intense review on the latest advancements of Earth Air Heat Exchangers *Renew Sustain Energy Rev*. **89** pp. 261–80

[20]   Hancock J F 2021 *Strawberries* 2nd Ed. Crop Production Science in Horticulture Series CABI

Acknowledgments